

## Magnetic Hardening of Nano-thick $\text{Sm}_2\text{Fe}_{17}\text{N}_x$ Films Grown by Pulsed Laser Deposition

Choong Jin Yang and Jianmin Wu<sup>1</sup>

*Electromagnetic Materials Lab., Research Institute of Industrial Science and Technology (RIST), P. O. Box 135, 790-330 Pohang, South Korea*

<sup>1</sup>*Dept. 2, Central Iron and Steel Research Institute, Beijing 100081, P. R. China*

(Received 7 September 2000)

$\text{Sm}_2\text{Fe}_{17}\text{N}_x$  film magnets were prepared using a  $\text{Sm}_2\text{Fe}_{17}$  target in a  $\text{N}_2$  gas atmosphere using a Nd-YAG pulsed laser ablation technique. The effect of nitrogen pressure, deposition temperature, pulse time and film thickness on the structure and magnetic properties of  $\text{Sm}_2\text{Fe}_{17}\text{N}_x$  film were studied. Increasing the nitrogen pressure up to 5 atm led to the formation of complete  $\text{Sm}_2\text{Fe}_{17}\text{N}_x$  compound. Optimized magnetic properties with the nitrogenation temperature in the range 500-530 °C could be obtained by extending the nitrogenation time up to 4 hours. Relatively low coercivities of 400-600 Oe were found in  $\text{Sm}_2\text{Fe}_{17}\text{N}_x$  films 50-100 nm thick, while a  $4\pi M_s$  of 10-12 kG could be achieved. In-plane anisotropy, which was the basic goal in this study, was achieved by controlling the nitrogenation parameters.

### 1. Introduction

There has been a recent boom in research on permanent magnet films, due to their potential use in microelectromechanical system (MEMS) and sensor applications. The permanent magnetic properties of the film magnets are a major concern in material selection. Many high-performance magnet films based on rare-earth transition compounds such as  $\text{SmCo}_5$  [1, 2],  $\text{Sm}(\text{Co},\text{M})_{7-8.5}$  [3-5],  $\text{Nd}_2\text{Fe}_{14}\text{B}$  [6, 7],  $\text{Nd}(\text{Fe},\text{Ti})_{12}\text{N}_x$  [8],  $\text{Sm}_2\text{Fe}_{17}\text{N}_x$  [9-12], and also nanocomposite films such as  $\text{Nd}_2\text{Fe}_{14}\text{B}/\alpha\text{-Fe}$  or  $\text{Fe}_3\text{B}$  [13-17], and  $\text{SmCo}_5/\text{Co}$  [18] have been studied extensively.

In this work, the magnetic properties of nanoscaled  $\text{Sm}_2\text{Fe}_{17}\text{N}_x$  films produced by laser ablation are reported. The effect of nitrogenation treatments such as  $\text{N}_2$  gas pressure during laser deposition, substrate temperature, laser pulsation time, and the effect of film thickness on the microstructure and magnetic properties of  $\text{Sm}_2\text{Fe}_{17}\text{N}_x$  films were studied. Most importantly, in-plane anisotropy must be induced in the nanoscale  $\text{Sm}_2\text{Fe}_{17}\text{N}_x$  films for the anticipated applications in MEMS or sensors, including the application for a biasing permanent magnet layer for a spin valve head in a high density recording hard disk drive. Accordingly, our attention was focused on the high performance permanent magnetic properties in the regime where an in-plane anisotropy can be developed. Since the target to be used is a rare earth compound single target, Nd-YAG laser pulsation was employed to make a high energy beam which permits rapid deposition.

### 2. Experiment

Nano-thick magnetic films of  $\text{SmFeN}$  were deposited by a Nd:YAG laser ablation technique. The laser beam energy density used in this study was about 200 J/cm<sup>2</sup>. For the ablation a single compound target of composition  $\text{Sm}_2\text{Fe}_{17}$  was used. The target was made by plasma arc melting and was subjected to a homogenization treatment. The nanoscale films were deposited on  $\text{SiO}_2$  glass at room temperature, and were annealed at 400-600 °C in a pressurized  $\text{N}_2$  gas atmosphere with pressure up to 5 atm for 1 to 4 hours. During the nitrogenation an external magnetic field of 10 kG was applied parallel to the plane of the film samples which was intended to develop magnetic anisotropy during the formation of the nitride phase. The film thickness was controlled ranging over 50-200 nm by controlling the number of laser pulses at a pulse rate of 10 Hz. An ' $\alpha$ -Step' measurement device was used to measure the thickness of the films. X-ray diffraction analysis ( $\text{Cu K}\alpha$ ) was used to identify the phases present, and the microstructure of films was characterized using high resolution TEM. A vibrating sample magnetometer was used to measure the magnetic properties of films in both the in-plane and perpendicular directions.

### 3. Results and Discussion

#### 3.1. Magnetic phase transformation

The target used in this study was confirmed to consist of single phase  $\text{Sm}_2\text{Fe}_{17}$  with very small amount of  $\alpha\text{-Fe}$ . Fig.

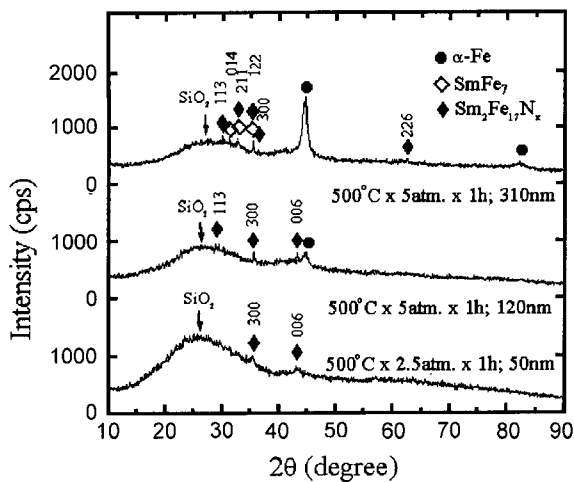


Fig. 1. X-ray diffraction patterns of  $\text{Sm}_2\text{Fe}_{17}\text{N}_x$  film with different thickness.

1 shows x-ray diffraction spectra of  $\text{Sm}_2\text{Fe}_{17}\text{N}_x$  films grown to different thicknesses. The nitrogenation condition for each sample is shown in the inset. No  $\alpha$ -Fe is detected in the 50 nm film. However,  $\alpha$ -Fe tends to form with increasing film thickness through 120 up to 310 nm. The magnetic phase present in the both 50 nm and 120 nm thick films was perfectly indexed to be  $\text{Sm}_2\text{Fe}_{17}\text{N}_x$ , while the films of 310 nm thick indicated the presence of both  $\text{Sm}_2\text{Fe}_{17}\text{N}_x$  and  $\text{SmFe}_7$  with no clear evidence of  $\text{Sm}_2\text{Fe}_{17}$  formation. Index-

ing was not conclusive since the  $\text{Sm}_2\text{Fe}_{17}\text{N}_x$  and  $\text{SmFe}_7$  phases show almost identical reflecting planes, as shown in Table 1 and 2, respectively. However, the coercivities of films with thicknesses more than 200 nm always showed low values of less than 60 Oe. These results might be due not only to the incomplete nitrogenation from  $\text{Sm}_2\text{Fe}_{17}$  to  $\text{Sm}_2\text{Fe}_{17}\text{N}_x$  but also to the presence of  $\text{SmFe}_7$  as is suggested by the x-ray pattern in Fig. 1.

In order to investigate the nitrogenation behavior of  $\text{Sm}_2\text{Fe}_{17}$ , a comparison of x-ray patterns for 50 nm thick films heat treated for 1 and 4 hours under 2.5 atm  $\text{N}_2$  atmosphere, respectively, was made as shown in Fig. 2. It can be noticed that the intensity of the diffraction peaks from the identical plane increases with the nitrogenation time. The transformation from  $\text{Sm}_2\text{Fe}_{17}$  to  $\text{Sm}_2\text{Fe}_{17}\text{N}_x$  would take time to be completed which is indicated by the intensity of reflected peaks. Since the best magnetic properties of  $\text{Sm}_2\text{Fe}_{17}\text{N}_x$  films were obtained after annealing around 500 °C in this study, the following discussion is focused only on the samples nitrogenated at 500 °C.

### 3.2. The effect of nitrogenation parameters on nano-thick $\text{Sm}_2\text{Fe}_{17}\text{N}_x$ films

The relationship between the magnetic properties of  $\text{Sm}_2\text{Fe}_{17}\text{N}_x$  films along in-plane direction and  $\text{N}_2$  pressure nitrogenated at 500 °C for 1 hour is shown in Fig. 3. It is clearly shown that the saturation magnetization ( $4\pi M_s$ ) and

Table 1. X-ray diffraction data indexed to  $\text{Sm}_2\text{Fe}_{17}\text{N}_x$  and  $\alpha$ -Fe

| No | X-ray diffraction Measurement Result |             |                  | $\text{Sm}_2\text{Fe}_{17}\text{N}_3$ |        |                  | $\alpha$ -Fe        |        |                  |
|----|--------------------------------------|-------------|------------------|---------------------------------------|--------|------------------|---------------------|--------|------------------|
|    |                                      |             |                  | JCPDS Standard Card                   |        |                  | JCPDS Standard Card |        |                  |
|    | d (Å)                                | 2θ (degree) | I/I <sub>0</sub> | hkl                                   | D (Å)  | I/I <sub>0</sub> | hkl                 | d (Å)  | I/I <sub>0</sub> |
| 1  | 3.0315                               | 29.440      | 100              | 113                                   | 3.0360 | 29               |                     |        |                  |
| 2  | 2.5253                               | 35.520      | 86               | 300                                   | 2.5240 | 39               |                     |        |                  |
| 3  | 2.0888                               | 43.280      | 83               | 006                                   | 2.1090 | 28               |                     |        |                  |
| 4  | 2.0214                               | 44.880      | 87               |                                       |        |                  | 110                 | 2.0268 | 100              |

Table 2. X-ray diffraction data indexed to  $\text{SmFe}_7$  and  $\alpha$ -Fe

| No | X-ray diffraction Measurement Result |             |                  | $\text{SmFe}_7$     |       |                  | $\alpha$ -Fe        |        |                  |
|----|--------------------------------------|-------------|------------------|---------------------|-------|------------------|---------------------|--------|------------------|
|    |                                      |             |                  | JCPDS Standard Card |       |                  | JCPDS Standard Card |        |                  |
|    | d (Å)                                | 2θ (degree) | I/I <sub>0</sub> | hkl                 | D (Å) | I/I <sub>0</sub> | hkl                 | d (Å)  | I/I <sub>0</sub> |
| 1  | 2.9761                               | 30.000      | 55               | 113                 | 2.969 | 65               |                     |        |                  |
| 2  | 2.8501                               | 31.360      | 52               | 014                 | 2.858 | 35               |                     |        |                  |
| 3  | 2.7282                               | 32.800      | 53               | 211                 | 2.725 | 16               |                     |        |                  |
| 4  | 2.5308                               | 35.440      | 48               | 122                 | 2.548 | 16               |                     |        |                  |
| 5  | 2.4715                               | 36.320      | 40               | 300                 | 2.465 | 65               |                     |        |                  |
| 6  | 2.1893                               | 41.200      | 41               |                     |       |                  |                     |        |                  |
| 7  | 2.0248                               | 44.720      | 100              |                     |       |                  | 110                 | 2.0268 | 100              |
| 8  | 1.8448                               | 49.360      | 32               |                     |       |                  |                     |        |                  |
| 9  | 1.5633                               | 59.040      | 29               |                     |       |                  |                     |        |                  |
| 10 | 1.4835                               | 62.560      | 29               | 226                 | 1.489 | 100              |                     |        |                  |
| 11 | 1.1732                               | 82.080      | 24               |                     |       |                  | 211                 | 1.1702 | 30               |

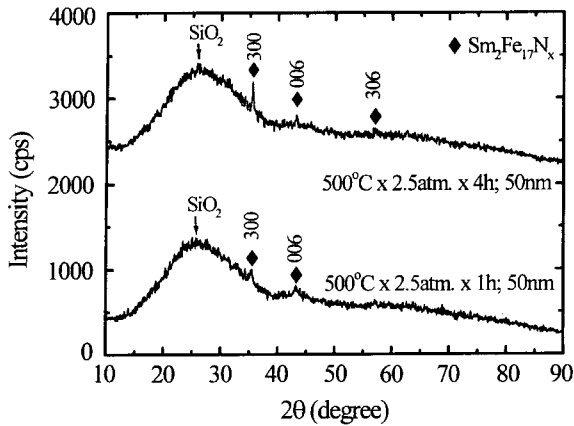


Fig. 2. X-ray diffraction patterns of  $\text{Sm}_2\text{Fe}_{17}\text{N}_x$  films treated with different nitrogenation times.

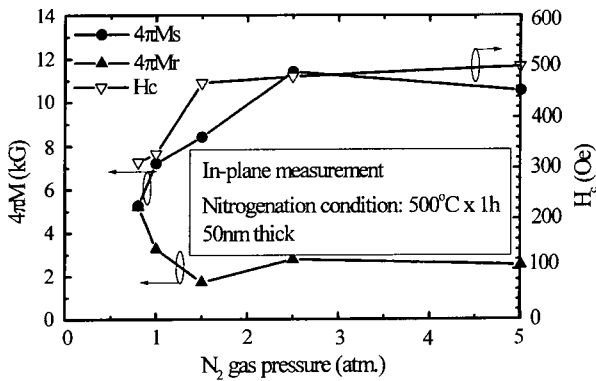


Fig. 3. Effect of  $\text{N}_2$  gas pressure on the magnetic properties along in-plane of films.

coercivity ( $H_c$ ) increase while the remanence ( $4\pi M_r$ ) decreases with increasing  $\text{N}_2$  gas pressure up to 2.5 atm. A low  $\text{N}_2$  pressure, nitrogenation makes the saturation magnetization and coercivity increase rapidly. However, both the saturation, remanent magnetization, and the coercivity become almost constant when the  $\text{N}_2$  gas pressure is higher than 2.5 atm. According to this result, the influence of  $\text{N}_2$  pressure, above a critical value seems not to be effective in the transformation from  $\text{Sm}_2\text{Fe}_{17}$  to  $\text{Sm}_2\text{Fe}_{17}\text{N}_x$  at  $500^\circ\text{C}$ . Comparison of hysteresis loops for samples treated at different  $\text{N}_2$  pressures was made, as shown in Fig. 4. As was expected, anisotropy along in-plane direction is prominent. The sample nitrogenated at 0.8 atm of  $\text{N}_2$  exhibits the character of a soft magnetic phase. This is because the  $\text{Sm}_2\text{Fe}_{17}$  phase seems not be transformed into  $\text{Sm}_2\text{Fe}_{17}\text{N}_x$  yet. However, the samples treated at 2.5 and 5 atm of  $\text{N}_2$  seem to show almost identical hysteresis. Consequently the  $M_r/M_s$  ratio was almost invariant.

The effect of film thickness on the magnetic properties along in-plane direction of the films processed at  $500^\circ\text{C}$  for 1 hour under 5 atm of  $\text{N}_2$  is shown in Fig. 5. Both the saturation ( $4\pi M_s$ ) and remanence ( $4\pi M_r$ ) increase up to 13 and 12 kG, respectively, with increasing the film thickness, while the coercivity decreases continuously to values below

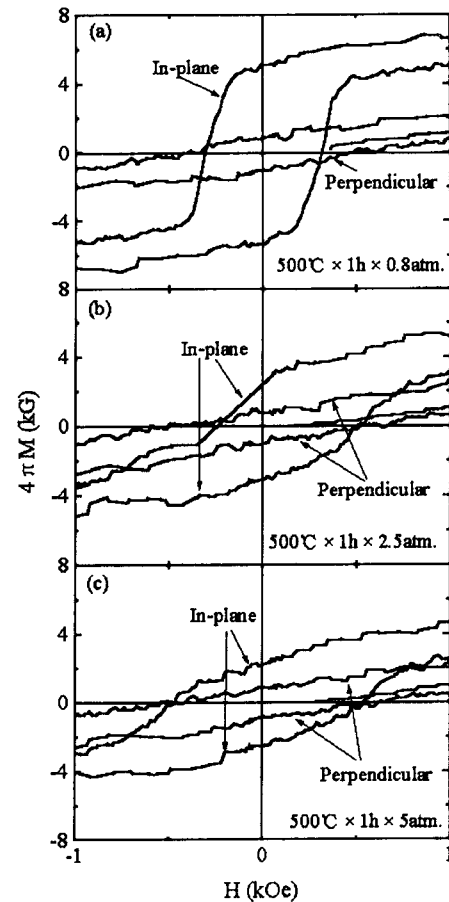


Fig. 4. Effect of  $\text{N}_2$  pressure on the hysteresis loop in-plane and perpendicular to the films 50 nm thick.

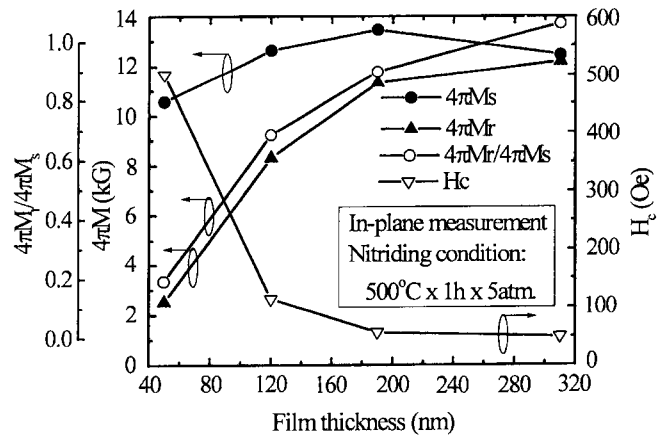


Fig. 5. Effect of film thickness on the in-plane magnetic properties.

100 Oe when the thickness is more than 120 nm. This means that the  $\text{Sm}_2\text{Fe}_{17}$  films hardly transform into  $\text{Sm}_2\text{Fe}_{17}\text{N}_x$  when the thickness is thicker than 120 nm. Above the thickness of 160 nm, the films were found to remain  $\text{Sm}_2\text{Fe}_{17}$  as indicated in Fig. 6(a) and (b). Analyzing the results exhibited in Fig. 5 and 6, one can notice that the  $4\pi M_r/4\pi M_s$  ratio, which is denoted by the open circles curve in Fig. 5, tends to increase with increasing the thickness. This is because the films tend to remain as  $\text{Sm}_2\text{Fe}_{17}$ ,

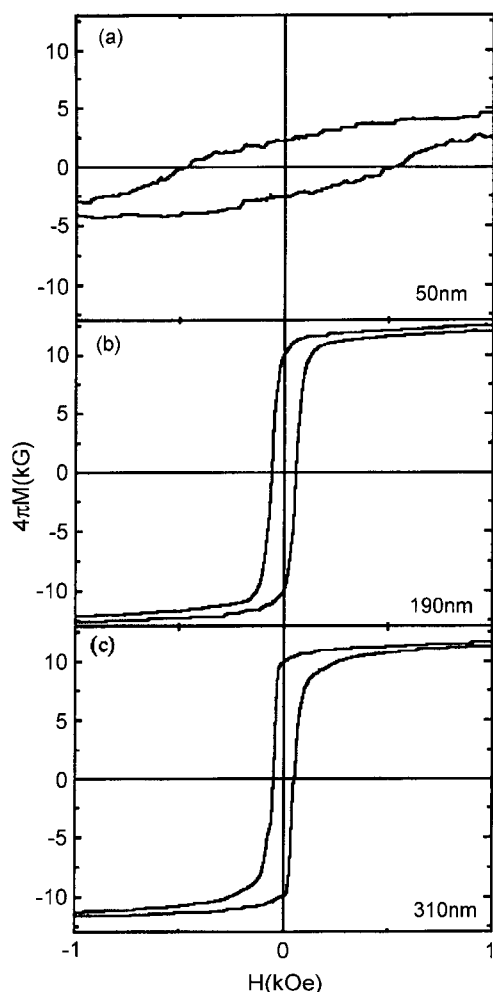


Fig. 6. Effect of film thickness on the in-plane hysteresis loop of films nitrogenated at 500 °C for 1 hr under 5 atm N<sub>2</sub>.

exhibiting a soft magnetic character.

The microstructure, or more precisely the crystallographic texture, of Sm<sub>2</sub>Fe<sub>17</sub>N<sub>x</sub> films could be dependent upon the thickness of films, which is also a function of deposition time. To study the effect of film thickness, i.e., the variation of texture, the films of 50 nm thick were treated at 500 °C under 2.5 atm of N<sub>2</sub> for various time periods, and the results are shown in Fig. 7. Before the nitrogenation takes place, 4πM<sub>s</sub> of the soft magnetic Sm<sub>2</sub>Fe<sub>17</sub> films shows a value around 9 kG, and 4πM<sub>r</sub> is rather low at about 5.5 kG, whereas the squareness should be high due to the soft magnetic character. Once nitrogenation occurs, the value of 4πM<sub>s</sub> increases due to the formation of Sm<sub>2</sub>Fe<sub>17</sub>N<sub>x</sub>, and 4πM<sub>r</sub> tends to decrease slowly due to the magnetic hardening. The coercivity increases abruptly from 100 Oe to 450 Oe after nitrogenation takes place. However, the high values of 4πM<sub>s</sub> and H<sub>c</sub> tend to drop after 1 hour, with a substantial variation in 4πM<sub>r</sub>. This means that textural change occurs with prolonged nitrogenation. To investigate the change of texture in detail, a comparison was made between in-plane and perpendicular measurement of films nitrogenated at 500 °C under 2.5 atm of N<sub>2</sub> for 2h and 4h,

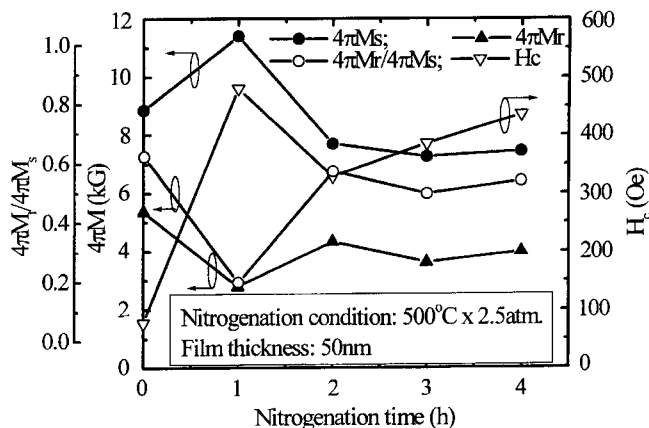


Fig. 7. Effect of nitrogenation time on the magnetic properties along in-plane of films.

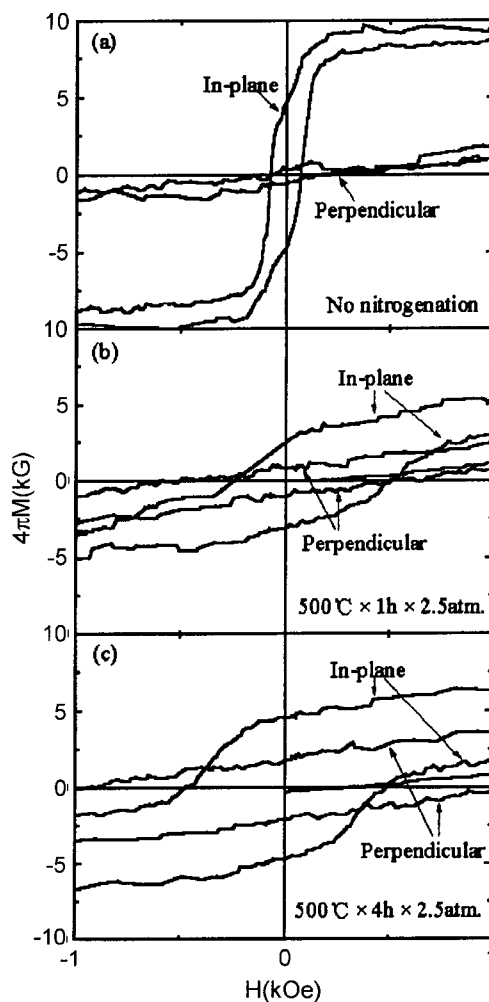


Fig. 8. Effect of nitrogenation time on the hysteresis loop in-plane and perpendicular to 50 nm films.

and a virgin Sm<sub>2</sub>Fe<sub>17</sub> sample, respectively, and the results are shown in Fig. 8. The virgin Sm<sub>2</sub>Fe<sub>17</sub> films, which initially showed in-plane anisotropy, tend to change their texture during nitrogenation, as shown in Fig. 8(b) and (c). With prolonged time of N<sub>2</sub> treatment the hysteresis curves measured in-plane tend to decrease in magnitude while the

curves measured in the perpendicular direction tend to show a large coercive field which is partly due to the change of texture. If Fig. 2 is examined carefully, the reflected intensity of the (003) plane is seen to become prominent after a prolonged nitrogenation time of 4 hours. Accordingly there must be some textural change with the duration of nitrogenation.

Fig. 9 shows the variation of coercivity measured along both in-plane and perpendicular to the film. Up to a thickness of 80 nm, coercivities along in-plane were larger than those in the perpendicular direction. However, this result was reversed with increasing film thickness due to the textural change, and the out-of plane anisotropy becomes prominent. Note that an external magnetic field was applied in-plane during the nitrogenation process to influence the magnetic anisotropy of the films. Of course applying an external field of 10 kG in the paramagnetic range of the  $\text{Sm}_2\text{Fe}_{17}\text{N}_x$  phase is expected to be ineffective. The magnetic anisotropy of films in the range up to 80 nm thick favored in-plane magnetization, as determined by repeated experiments.

Recently, there have been many research reports on the effects of high magnetic fields about 10 Tesla applied to Fe-based alloy steel [19, 20]. This externally applied field along a certain direction facilitated the textural formation of ultra fine (about 1  $\mu\text{m}$ ) ferrite grains along the field direction. The mechanism was explained to be due to the reduction in diffusion speed of Fe atoms in the range of increased magnetic transformation temperature from ferrite( $\alpha$ ) to austenite( $\gamma$ )s by the applied magnetic field. Accordingly, we believe that the in-plane anisotropy induced by the applied field in films up to 80 nm thick was caused by the same effect. As shown in Fig. 9, taking into account the abrupt drop of the coercivity with increasing the film thickness, the induced anisotropy might be due to the applied magnetic field, not by the shape anisotropy. Fig. 10 shows the typical nano-scaled microstructure of films nitrogenated at 500 °C

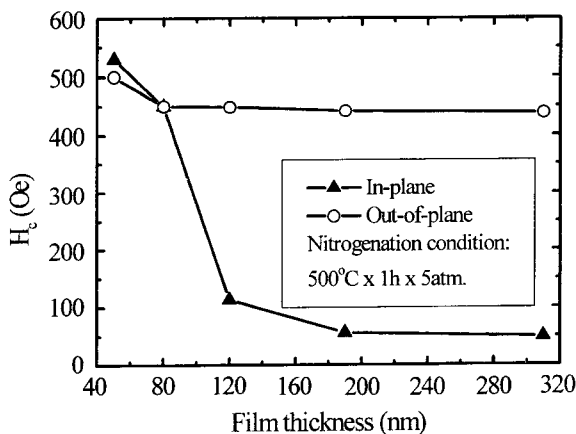


Fig. 9. Effect of film thickness on the coercivity in-plane and perpendicular to the film.

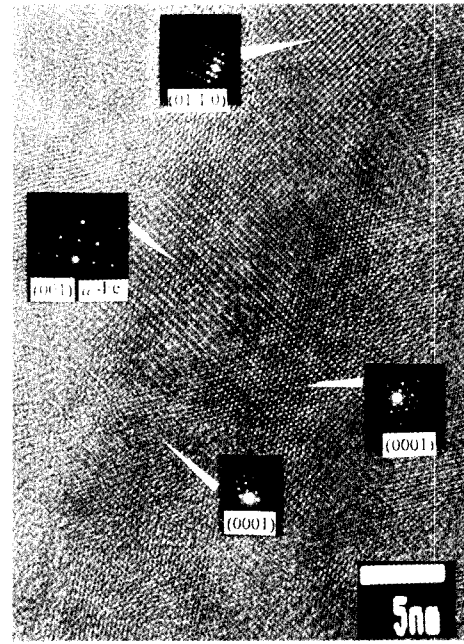


Fig. 10. Typical high resolution TEM microscope of the sample nitrogenated at 500 °C for 4 hours under 2.5 atm of  $\text{N}_2$ .

for 4 hours under  $\text{N}_2$  pressure of 2.5 atm. Basically (001)  $\text{Sm}_2\text{Fe}_{17}\text{N}_x$  grains are shown to be prominent as was suggested in Fig. 2 and Fig. 9. However, (010)  $\text{Sm}_2\text{Fe}_{17}\text{N}_x$  and (001) Fe grains are also shown to be present around the center region.

### Summary

$\text{Sm}_2\text{Fe}_{17}\text{N}_x$  film magnets were grown by a laser ablation technique using a single  $\text{Sm}_2\text{Fe}_{17}$  target. Nitrogen pressure and deposition temperature were found to be very influential on the nitrogenation of  $\text{Sm}_2\text{Fe}_{17}$  films into  $\text{Sm}_2\text{Fe}_{17}\text{N}_x$ . In addition, the deposition time (i.e., the film thickness) was shown to be decisive on the development of anisotropic texture in  $\text{Sm}_2\text{Fe}_{17}\text{N}_x$  films. By controlling the  $\text{N}_2$  pressure from 1 to 4 atm and the nitriding temperature at about 500~530 °C, an in-plane anisotropy was obtainable in the films up to 80 nm thick with the aide of an externally applied magnetic field. However, the in-plane anisotropy changes to out-of-plane due to the textural change in thicker films.  $\text{Sm}_2\text{Fe}_{17}\text{N}_x$  films with  $4\pi M_s$  of 13 kG,  $4\pi M_r$  of 12 kG, or coercivity ( $H_c$ ) of 550 Oe were obtained by an optimized nitrogenation treatment although not all three values could be obtained in the same sample. However, an  $H_c$  of 550 Oe is still low compared to that of bulk  $\text{Sm}_2\text{Fe}_{17}\text{N}_3$ . One of the reasons for the low values was found to be the oxidation of films during the laser ablation of  $\text{Sm}_2\text{Fe}_{17}$  films, which was very difficult to avoid. Also the presence of  $\text{SmFe}_7$  phase, which was not clearly distinguished from the  $\text{Sm}_2\text{Fe}_{17}\text{N}_x$  phase, might also be a reason why the films exhibited relatively low values of coercivity.

## Acknowledgement

The authors would like to express thanks for support from The Research Center for Advanced Magnetic Materials at Chungnam National University under Contract No. of 2000D004, and from The Korean Ministry of Science & Technology under contract No. of 99E006, to carry out the present study.

## References

- [1] F. J. Cadieu, T. D. Cheung, S. H. Aly, L. Wickramasekara, and R. C. Pirich, IEEE Trans. on Magn. **Mag-19**, 2038 (1983).
- [2] F. J. Cadieu, R. Rain, T. Theodoropoulos, and Li Chen, J. Appl. Phys. **85**, 5895 (1999).
- [3] H. Hegde, S. U. Jen, K. Chen, and F. J. Cadieu, J. Appl. Phys. **73**, 5926 (1993).
- [4] V. Neu and S. A. Shaheen, J. Appl. Phys. **86**, 7006 (1999).
- [5] F. J. Cadieu, H. Hegde, and K. Chen, IEEE Trans. on Magn. **Mag-25**, 3788 (1989).
- [6] Choong Jin Yang, Sang Won Kim, and Jong Seog Kang, J. Appl. Phys. **83**, 6620 (1998).
- [7] J. L. Tsai, E. Y. Huang, T. S. Chin, and S. K. Chen, IEEE Trans. on Magn. **Mag-33**, 3646 (1997).
- [8] A. Navarathna, H. Hegde, R. Rani, K. Chen, and F. J. Cadieu, IEEE Trans. on Magn. **Mag-29**, 2812 (1993).
- [9] P. W. Jang, D. Wang, and W. D. Doyle, J. Appl. Phys. **81**, 4664 (1997).
- [10] D. Wang, G. C. Hadjipanayis, and D. J. Sellmyer, IEEE Trans. on Magn. **Mag-28**, 2590 (1992).
- [11] R. Rnai, H. Hegde, A. Navarathna, and F. J. Cadieu, J. Appl. Phys. **73**, 6023 (1993).
- [12] Jae Man Song, Hiroyuki Sadakata, Masaki Nakano, Yasuhisa Kanai, Hirotoshi Fukunaga, and Jae Gui Koh, IEEE Trans. on Magn. **Mag-35**, 3052 (1999).
- [13] Choong Jin Yang and Song Won Kim, J. Magn. Magn. Mater. **202**, 311 (1999).
- [14] Choong Jin Yang and Eon Byung Park, J. Magn. Magn. Mater. **168**, 278 (1997).
- [15] Choong Jin Yang and Eon Byung Park, J. Magn. Magn. Mater. **166**, 243 (1997).
- [16] Youhui Gao, Jinghan Zhu, Yuqing Weng, Eon Byung Park, and Choong Jin Yang, J. Magn. Magn. Mater. **191**, 146 (1999).
- [17] Youhui Gao, Jinghan Zhu, Choong Jin Yang and Eon Byung Park, J. Magn. Magn. Mater. **186**, 97 (1998).
- [18] J. P. Liu, R. Skomski and D. J. Sellmyer, J. Appl. Phys. **85**, 4812 (1999).
- [19] J. of Japanese Institute of Metal (Special Issue on materials Behavior under High Magnetic Field), **61**, 1271 (1997).
- [20] M. Shimotomai, CAMP-ISIJ, 126 (1998).